



HAL
open science

Nanosecond UV laser-induced fatigue effects in the bulk of synthetic fused silica: a multi-parameter study

Céline Gouldieff, Frank R. Wagner, Jean-Yves Natoli

► To cite this version:

Céline Gouldieff, Frank R. Wagner, Jean-Yves Natoli. Nanosecond UV laser-induced fatigue effects in the bulk of synthetic fused silica: a multi-parameter study. *Optics Express*, 2015, 23 (3), pp.2962-2972. 10.1364/OE.23.002962 . hal-01220018

HAL Id: hal-01220018

<https://amu.hal.science/hal-01220018v1>

Submitted on 27 Oct 2015

HAL is a multi-disciplinary open access archive for the deposit and dissemination of scientific research documents, whether they are published or not. The documents may come from teaching and research institutions in France or abroad, or from public or private research centers.

L'archive ouverte pluridisciplinaire **HAL**, est destinée au dépôt et à la diffusion de documents scientifiques de niveau recherche, publiés ou non, émanant des établissements d'enseignement et de recherche français ou étrangers, des laboratoires publics ou privés.

Nanosecond UV laser-induced fatigue effects in the bulk of synthetic fused silica: a multi-parameter study

Céline Gouldieff,^{1,2} Frank Wagner,^{1,*} and Jean-Yves Natoli¹

¹ Aix-Marseille Université, CNRS, Centrale Marseille, Institut Fresnel UMR 7249, 13013 Marseille, France

² Currently with the Institut de Physique de Rennes UMR CNRS 6251, Université de Rennes 1, 35042 Rennes, France
[*frank.wagner@fresnel.fr](mailto:frank.wagner@fresnel.fr)

Abstract: Multiple-pulse S-on-1 laser damage experiments were carried out in the bulk of synthetic fused silica at 355 nm and 266 nm. Two beam sizes were used for each wavelength and the pulse duration was 8 ns. The results showed a fatigue effect that is due to cumulative material modifications. The modifications have a long lifetime and the fatigue dynamics are independent of the used beam sizes but differ for the two wavelengths. Based on the fact that, in the context of material-modification induced damage, the damage thresholds for smaller beams are higher than for larger beams, we discuss possible mechanisms of damage initiation.

©2015 Optical Society of America

OCIS codes: (140.3330) Laser damage; (140.3440) Laser-induced breakdown; (160.6030) Silica; (160.2750) Glass and other amorphous materials; (160.4670) Optical materials.

References and links

1. G. J. Exarhos, D. Ristau, M. J. Soileau, C. J. Stolz, and V. E. Gruzdev, eds., *Proceedings of Boulder Damage Symposium and Proceedings of SPIE Laser Damage Conferences*, Proc. SPIE (1969–2014).
2. N. Leclerc, C. Pfeleiderer, J. Wolfrum, K. Greulich, W. P. Leung, M. Kulkarni, and A. C. Tam, “Transient absorption and fluorescence spectroscopy in fused-silica induced by pulsed KrF excimer laser irradiation,” *Appl. Phys. Lett.* **59**(26), 3369–3371 (1991).
3. N. Leclerc, C. Pfeleiderer, H. Hitzler, J. Wolfrum, K. O. Greulich, S. Thomas, H. Fabian, R. Takke, and W. Englisch, “Transient 210-nm absorption in fused silica induced by high-power UV laser irradiation,” *Opt. Lett.* **16**(12), 940–942 (1991).
4. D. J. Krajnovich, I. K. Pour, A. C. Tam, W. P. Leung, and M. V. Kulkarni, “Sudden onset of strong absorption followed by forced recovery in KrF laser-irradiated fused silica,” *Opt. Lett.* **18**(6), 453–455 (1993).
5. M. A. Stevens-Kalceff, A. Stesmans, and J. Wong, “Defects induced in fused silica by high fluence ultraviolet laser pulses at 355 nm,” *Appl. Phys. Lett.* **80**(5), 758–760 (2002).
6. L. Gallais, J. Capoulade, F. Wagner, J. Y. Natoli, and M. Commandre, “Analysis of material modifications induced during laser damage in SiO₂ thin films,” *Opt. Commun.* **272**(1), 221–226 (2007).
7. M. Schillinger, D. Morancais, F. Fabre, and A. Culoma, “ALADIN: The LIDAR instrument for the AEOLUS mission,” *Proc. SPIE* **4881**, 40–51 (2003).
8. O. N. Bosyi and O. M. Efimov, “Relationships governing the cumulative effect and its mechanism in the absence of subthreshold ionisation of a glass matrix,” *Quantum Electron.* **26**(8), 718–723 (1996).
9. O. N. Bosyi and O. M. Efimov, “Relationships governing the cumulative effect and its mechanism under conditions of multiphoton generation of colour centres,” *Quantum Electron.* **26**(8), 710–717 (1996).
10. A. E. Chmel, “Fatigue laser-induced damage in transparent materials,” *Mat. Sci. Eng. B. Solid.* **49**(3), 175–190 (1997).
11. L. Gallais, J. Y. Natoli, and C. Amra, “Statistical study of single and multiple pulse laser-induced damage in glasses,” *Opt. Express* **10**(25), 1465–1474 (2002).
12. F. R. Wagner, G. Duchateau, J.-Y. Natoli, H. Akhouayri, and M. Commandre, “Catastrophic nanosecond laser induced damage in the bulk of potassium titanyl phosphate crystals,” *J. Appl. Phys.* **115**(24), 243102 (2014).
13. S. C. Jones, P. Braunlich, R. T. Casper, X. A. Shen, and P. Kelly, “Recent progress on laser-induced modifications and intrinsic bulk damage of wide-gap optical-materials,” *Opt. Eng.* **28**(10), 281039 (1989).
14. X. Ling, “Nanosecond multi-pulse damage investigation of optical coatings in atmosphere and vacuum environments,” *Appl. Surf. Sci.* **257**(13), 5601–5604 (2011).
15. F. R. Wagner, C. Gouldieff, and J.-Y. Natoli, “Contrasted material responses to nanosecond multiple-pulse laser damage: From statistical behavior to material modification,” *Opt. Lett.* **38**(11), 1869–1871 (2013).
16. M. Cannas and F. Messina, “Nd: Yag laser induced E' centers probed by in situ absorption measurements,” *J. Non-Cryst. Solids* **351**(21-23), 1780–1783 (2005).
17. A. Burkert and U. Natura, “353 nm high fluence irradiation of fused silica,” *Proc. SPIE* **7132**, 71321Q (2008).

18. L. Lamaignère, S. Bouillet, R. Courchinoux, T. Donval, M. Josse, J. C. Poncetta, and H. Bercegol, "An accurate, repeatable, and well characterized measurement of laser damage density of optical materials," *Rev. Sci. Instrum.* **78**(10), 103105 (2007).
19. L. Gallais and J. Y. Natoli, "Optimized metrology for laser-damage measurement: Application to multiparameter study," *Appl. Opt.* **42**(6), 960–971 (2003).
20. International Organization for Standardization, "Lasers and laser-related equipment. Test methods for laser-induced damage threshold. Part 2: Threshold determination," (**ISO 21254-2**, 2011).
21. F. R. Wagner, A. Hildenbrand, H. Akhouayri, C. Gouldieff, L. Gallais, M. Commandré, and J.-Y. Natoli, "Multipulse laser damage in potassium titanyl phosphate: Statistical interpretation of measurements and the damage initiation mechanism," *Opt. Eng.* **51**(12), 121806 (2012).
22. A. Melninkaitis, J. Mirauskas, M. Jupé, D. Ristau, J. W. Arenberg, and V. Sirutkaitis, "The effect of pseudo-accumulation in the measurement of fatigue laser-induced damage threshold," *Proc. SPIE* **7132**, 713203 (2008).
23. L. G. DeShazer, B. E. Newnam, and K. M. Leung, "Role of coating defects in laser-induced damage to dielectric thin films," *Appl. Phys. Lett.* **23**(11), 607 (1973).
24. L. Jensen, S. Schrameyer, M. Jupé, H. Blaschke, and D. Ristau, "Spotsize dependence of the LIDT from the NIR to the UV," *Proc. SPIE* **7504**, 75041E (2009).
25. J. O. Porteus and S. C. Seitel, "Absolute onset of optical surface damage using distributed defect ensembles," *Appl. Opt.* **23**(21), 3796–3805 (1984).
26. J. Y. Natoli, L. Gallais, H. Akhouayri, and C. Amra, "Laser-induced damage of materials in bulk, thin-film, and liquid forms," *Appl. Opt.* **41**(16), 3156–3166 (2002).
27. A. Hildenbrand, F. R. Wagner, H. Akhouayri, J.-Y. Natoli, and M. Commandré, "Accurate metrology for laser damage measurements in nonlinear crystals," *Opt. Eng.* **47**(8), 083603 (2008).
28. E. Eva and K. Mann, "Calorimetric measurement of two-photon absorption and color-center formation in ultraviolet-window materials," *Appl. Phys. A: Mater.* **62**, 143–149 (1996).
29. K. Arai, H. Imai, H. Hosono, Y. Abe, and H. Imagawa, "2-photon processes in defect formation by excimer lasers in synthetic silica glass," *Appl. Phys. Lett.* **53**(20), 1891–1893 (1988).
30. K. Saito and A. J. Ikushima, "Absorption edge in silica glass," *Phys. Rev. B* **62**(13), 8584–8587 (2000).
31. L. Skuja, "Optically active oxygen-deficiency-related centers in amorphous silicon dioxide," *J. Non-Cryst. Solids* **239**(1-3), 16–48 (1998).
32. N. Kuzuu, K. Yoshida, H. Yoshida, T. Kamimura, and N. Kamisugi, "Laser-induced bulk damage in various types of vitreous silica at 1064, 532, 355, and 266 nm: Evidence of different damage mechanisms between 266-nm and longer wavelengths," *Appl. Opt.* **38**(12), 2510–2515 (1999).
33. D. W. Bäuerle, *Laser Processing and Chemistry*, 4th ed., Advanced Texts in Physics (Springer, 2011).
34. Heraeus Quarzglas GmbH & Co. KG, "Quartz glass for optics - data and properties" (2013), retrieved 2014, http://heraeus-quarzglas.com/media/webmedia_local/downloads/broschren_mo/dataandproperties_optics_fusedsilica.pdf.
35. G. Duchateau, "Simple models for laser-induced damage and conditioning of potassium dihydrogen phosphate crystals by nanosecond pulses," *Opt. Express* **17**(13), 10434–10456 (2009).
36. E. L. Dawes and J. H. Marburger, "Computer studies of self-focusing," *Phys. Rev.* **179**(3), 862–868 (1969).
37. H. Li, F. Zhou, X. Zhang, and W. Ji, "Bound electronic kerr effect and self-focusing induced damage in second-harmonic-generation crystals," *Opt. Commun.* **144**(1-3), 75–81 (1997).

1. Introduction

Synthetic fused silica is the best-performing amorphous optical material in terms of laser-induced damage at wavelengths close to 1 μm and a large number of laser damage studies has been published [1]. Using this high quality optical material for UV-applications, high OH content synthetic fused silica (wet fused silica), as for example Suprasil I (Heraeus) that was used in the current study, was found to be the best choice. The first studies of synthetic fused silica in the UV range mostly aimed at low-fluence applications like exposure of photosensitive polymers for microelectronics fabrication. These studies, carried out at excimer laser wavelengths, revealed that high OH-content synthetic fused silica from different manufacturers may show significant differences in terms of laser-induced absorption [2, 3]. Two types of defects, Non-bridging oxygen hole centers (NBOHC) and E' centers were observed by absorption and luminescence measurements [2]. Using separated bursts of laser pulses, it was shown that the two defect types do not exist independently, but that one might be converted to the other [3, 4]. The same defects were also found when studying the surrounding of laser damage craters generated by intense laser irradiation [5, 6].

More recently, high UV-fluences can be generated by frequency conversion of solid state lasers emitting close to 1 μm wavelength and important space projects using these lasers are realized [7] generating a need to understand multi-pulse laser damage issues. Indeed, it was observed in various optical materials that multi-pulse irradiation leads to a decrease of the laser-induced damage threshold with increasing number of pulses. This effect is commonly

named “fatigue” effect and was observed in glasses [8–11], in crystals [12, 13], and in optical coatings [14]. Few studies exist that use experimental evidence to develop a physical image of the material modifications operated by nanosecond UV-irradiation and explaining the reduced laser-damage threshold ([8, 9, 13] and references in [10]). These studies use other wavelengths and other materials than the ones we report on here.

In a previous work [15], we described a method allowing to discriminate the two possible cases of fatigue encountered: statistical pseudo-fatigue, related to the fact that the higher the number of shots, the more probably the material will damage, and fatigue due to cumulative material modifications. Our study showed that synthetic fused silica (Suprasil 1) irradiated in the bulk showed a fatigue effect that was due to statistical pseudo-fatigue when irradiated at 1064 nm while the fatigue effect at 355 nm came from cumulative material modifications.

The current work presents more detailed measurements carried out at 355 nm and 266 nm in the bulk of Suprasil 1 using two different beam sizes for each wavelength. One may mention that at these wavelengths no laser-induced absorption could be evidenced in synthetic fused silica, even at very high pulse numbers [16, 17].

2. Experimental details

The tested Suprasil 1 samples had a diameter of 38.1 mm, a thickness of 9.525 mm and they were standard polished on both sides. Relatively thick samples were chosen to avoid surface damage that may appear during the bulk damage tests with weakly focused laser beams. The beam focus was placed in the middle of the sample thickness.

A sketch of the laser damage test setup is shown in Fig. 1. The laser source is a Spectra Physics Lab series laser (frequency converted Nd:YAG laser) operating at 50 Hz pulse repetition rate. The pulse duration is approximately 8 ns (full width at half maximum) for both used wavelengths: 355 nm and 266 nm. The system was not injection seeded for these experiments because a check for reliable mono-mode operation on a pulse-to-pulse basis was not possible at 50 Hz pulse repetition rate. Moreover, previous experiments did not show an influence of longitudinal multi-mode operation [15].

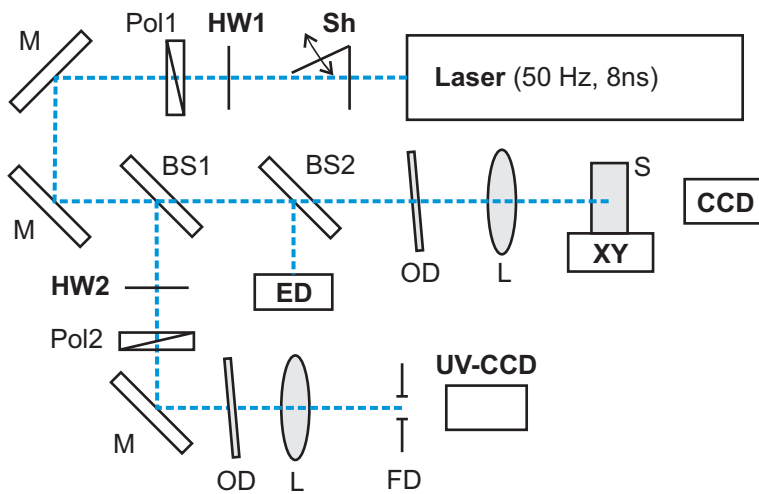
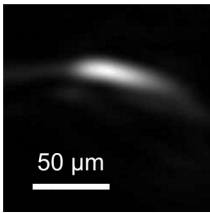
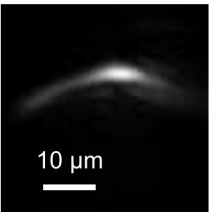
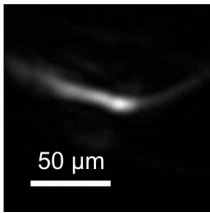
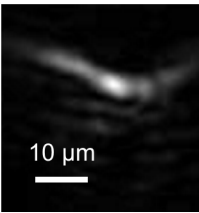


Fig. 1. Schematic view of the used setup. Elements in bold face communicate with the computer for automation of the experiment. Sh: fast mechanical shutter, HW: half wave plates, Pol: high power Glan-Taylor polarizers, M: mirrors, BS: beam splitters, ED: pyroelectric energy detector, OD: attenuation filters, L: two identical lenses, XY: x-y positioning stage for the sample S, CCD: in situ damage detection camera with microscope objective and laser blocking filter, FD: field diaphragm used to align the UV-CCD camera that acquires the beam profiles.

S-on-1 damage probability measurements with recording of the number of shots at which damage occurs (N_D) were carried out using two different beam sizes at both wavelengths. The

maximum number of pulses per site was 10^4 . The spatial beam profile at the focus was not close to Gaussian and the details are given in Fig. 2.

The setup is fully automated in a LabView environment. Two triggered fast digital cameras (> 100 fps) combined with suited microscope objectives are used for in situ damage detection (CCD in Fig. 1) and beam profile recording (UV-CCD) on a shot-to-shot basis. The optical path from beam splitter (BS1) to the sample (S) is the same as to the field diaphragm (FD) of the beam profile camera and identical lenses (L) were used for focusing in both arms of the setup. To choose the set of fluence to test on the different sites of the sample, an attenuator (HW1 / Pol1) was used. Moreover, to ensure well-exposed beam profile images for all settings, a second attenuator was positioned in front of the beam profile camera and coordinated with HW1 / Pol1 with LabView [18]. All beam profile images were saved in real-time on the computer and used after the experiment to determine the statistical uncertainty of the mean peak fluence for each site and each irradiation condition (see Fig. 2). The reference energy values measured by the pyroelectric detector were stored in the local memory of the detector during the test of each site and transferred to the computer afterwards. In situ damage detection was performed by simple image processing [19]. Camera exposure, image readout, image processing, image saving and the feedback to the shutter had to be accomplished within the 20 ms period between two laser pulses. In general this was possible to achieve on the used computer, except at the very beginning of the irradiation. Thus, single pulse testing cannot be directly carried out using this setup configuration. The minimum detectable pulse number is approximately 2 or 3. Once damage was detected, the mechanical shutter was closed and the reference energies were transferred to the computer. The number of energies corresponds to the number of pulses that were necessary to damage the site (N_D).

Wavelength	355 nm		266 nm	
Diameter*	40 μm	8.9 μm	30 μm	11.5 μm
Typical beam profile				
Effective area	$1.0 \cdot 10^{-5} \text{ cm}^2$	$6.8 \cdot 10^{-7} \text{ cm}^2$	$5.7 \cdot 10^{-6} \text{ cm}^2$	$1.1 \cdot 10^{-6} \text{ cm}^2$
σ_F / \bar{F} for a single site**	3.7 %	6.8 %	8.3 %	7.5 %
σ_F / \bar{F} for a group of sites**	3.9 %	7.9 %	9.1 %	8.1 %

* $1/e^2$ -diameter of a Gaussian beam with same peak fluence and same surface at $1/e$ of the peak fluence.

** Standard deviation divided by mean, as deduced from the variation of the brightest pixel of the beam profile images.

Fig. 2. Characterization of the different test beams.

All damaged sites were manually checked ex-situ after the test according to ISO 21254-2 using a microscope in differential interference contrast mode [20]. This allowed eliminating from the statistics the sites that were stopped to be irradiated not due to damage but due to noise on the damage detection camera and the sites that were detected as undamaged by the online damage detection but that were nevertheless damaged.

For each site we thus know if it was damaged or not, and, if damage occurred, we also know the pulse number N_D at which the site was damaged. The pulse energies, together with the effective area of the used beam profile, give access to the average fluence F used on each site. Grouping sites with similar fluences allows then to obtain the damage probabilities $P(F,S)$. For example, to estimate the 2200-on-1 damage probability at approximately 25 J/cm^2 (Fig. 3), only sites having a fluence close to 25 J/cm^2 are used (11 sites). We then check how many of these sites have an N_D of 2200 or less (4 sites) and the best estimate for the corresponding damage probability is $P(25 \text{ J/cm}^2, 2200) = 4/11$. Knowing the damaging pulse number N_D for each site thus enables us to obtain detailed P(S)-data as shown in Fig. 3 for example.

3. Material-modification dominated damage initiation

The fatigue effect is defined as a decrease of the S-on-1 damage threshold with increasing pulse number S . This effect can be caused by two mechanisms (i) accumulating material modifications operated by the incubation pulses or (ii) a statistical effect due to the measurement protocol [15]. The statistical model assumes a constant single pulse damage probability p_1 for all pulses at a given fluence, meaning that the successive shots are considered as independent. It thus excludes material modifications during the irradiation. As the S-on-1 damage probability $P(S)$ is defined by damages that occur at pulse number S or before, the complement, $1 - P(S)$, is given by the event that no damage occurred during the first S pulses. Thus, for constant p_1 , one expects according to the statistical model:

$$1 - P(S) = (1 - p_1)^S \quad (1)$$

Mainly two different processes may be at the origin of the single pulse damage probability p_1 with $0 < p_1 < 1$: laser fluctuations [21, 22] or stochastic laser/matter-interaction [12, 15]. In both cases the P(S)-curves will have the same shape given by Eq. (1) and illustrated in Fig. 3.

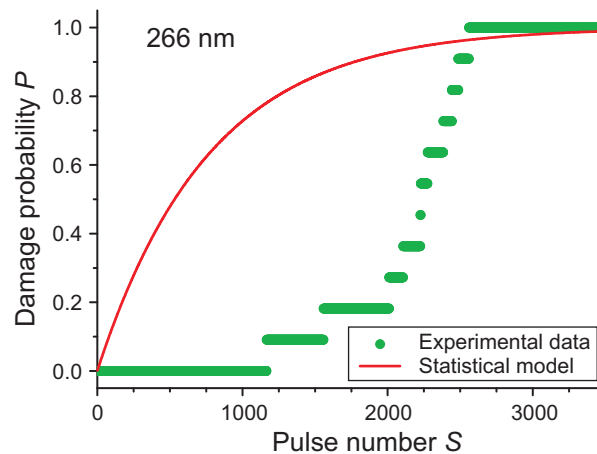


Fig. 3. Example of a $P(S)$ -curve (green dots) extracted from a 5000-on-1 measurement using 11 different sites. Wavelength, peak fluence and beam diameter were 266 nm, 24.8 J/cm^2 and $11.5 \mu\text{m}$ respectively. The red line is obtained from the statistical model for a comparable situation ($P \approx 1$ reached at similar pulse number S). The mismatch between data and model indicates that material modifications caused the fatigue effect at this wavelength and that laser fluctuations do not dominate the measured fatigue behavior.

As mentioned before, multiple-pulse laser-induced damage at the UV wavelengths 355 nm and 266 nm is dominated by the accumulation of light-induced material modifications in the bulk of fused silica. Contrary to what can be observed at 1064 nm [14, 15, 21] the statistical model cannot describe the damage probability as a function of the used laser pulses for all

tested fluences. An example of this mismatch is shown in Fig. 3 for 266 nm irradiation and a similar plot at 355 nm is given in [15].

The difference of the $P(S)$ -data from the statistical model also shows that the measurement is not dominated by any other statistical process linked to the laser pulses, in particular laser fluctuations. It has been shown for example that a bad pointing stability of the laser beam can theoretically generate statistical pseudo-fatigue [22]. The same is true for depointing combined with pulse energy fluctuations [21, 22] and intensity fluctuations due to the longitudinal multi-mode operation of the laser. The fact that the fatigue is not of the statistical type thus indicates that the physics of the material modification prevails over all statistical influences. In particular, this shows that laser fluctuations (directional stability, pulse energy, temporal profile and spatial profile) are not responsible for the multiple pulse laser damage in our measurement conditions.

In fact, if the sample is perfectly homogeneous, the laser perfectly stable and the process of material modification deterministic, the generation of the light induced defects will be perfectly reproducible. At a given set of irradiation parameters (fluence, beam size etc.) the critical defect density leading to damage initiation during the next pulse will always be reached after the same number of incubation pulses. Thus a step function in the $P(S)$ representation is expected in this idealized situation. The fact that the experimental $P(S)$ -curve is not a step function is mainly caused by the above-mentioned laser instabilities that widen the distribution of pulse numbers observed to cause damage at a given fluence. Moreover, the long steps for which the probability is not equal to zero in Fig. 3 may indicate the presence of rare weak sites in sample. In fact, although the material is considered as homogeneous and the tested sites are considered identical in terms of laser-damage threshold, some rare sites that are weaker than average can exist because of structural defects, bubbles, inclusions etc.

The presented $P(S)$ curve (Fig. 3), obtained for relatively weak fluence clearly indicates a fatigue that is not dominated by statistical aspects. However, for higher fluence values, it may be difficult to distinguish damage initiated by laser-induced material modifications from statistical pseudo-fatigue. Indeed, damage occurs much more rapidly inducing a small number of data in the $P(S)$ representation. To conclude on the type of fatigue, one has thus to take into account the whole set of $P(S)$ curves at given laser spot size and wavelength, and in particular to examine carefully the $P(S)$ curves obtained at low fluences.

4. Fatigue dynamics

Operating at a constant pulse repetition rate, the number of pulses required to damage the material, N_D , represents also the time requested for the material to damage. The $N_D(F)$ graph thus gives access to the “dynamics” of the fatigue process for a given material and given laser parameters (wavelength, beam size...). For better comparison of the fatigue dynamics related to different laser parameters, the fluence of each data set is usually normalized.

The striking feature of the data of Bosyi and Efimov [8, 9] is the fact that their fatigue dynamics data is different at different laser spot sizes. They showed that this can be understood considering that the material changes induced by the early pulses (compaction or color center generation) influence the propagation properties of the next pulse, focusing it to higher fluences than the early pulses.

Figure 4 shows the $N_D(F_{\text{norm}})$ representation of our data for both wavelengths and both beam sizes used at each wavelength. As single pulse damage is not directly accessible with the used setup, we normalized the data arbitrarily to the 50% damage threshold for 500 pulses.

In contrast to the data of Bosyi and Efimov, our data superpose perfectly at both wavelengths and for laser beam diameters similar to theirs (in the range of 10 to 40 μm). In conclusion, beam propagation aspects do not play a major role in the accumulation mechanism in Suprasil 1 for our experimental conditions.

Considering closely both semi-logarithmic graphs depicted in Fig. 4, one can evidence in each of them two domains of normalized fluence that seem to follow linear laws (see dashed straight lines in Fig. 4). Moreover, one may notice that the slopes of the lines for the high-

fluence range are identical for both wavelengths. As for the lines obtained in the low-fluences range, the slope is stronger at 355 nm than at 266 nm.

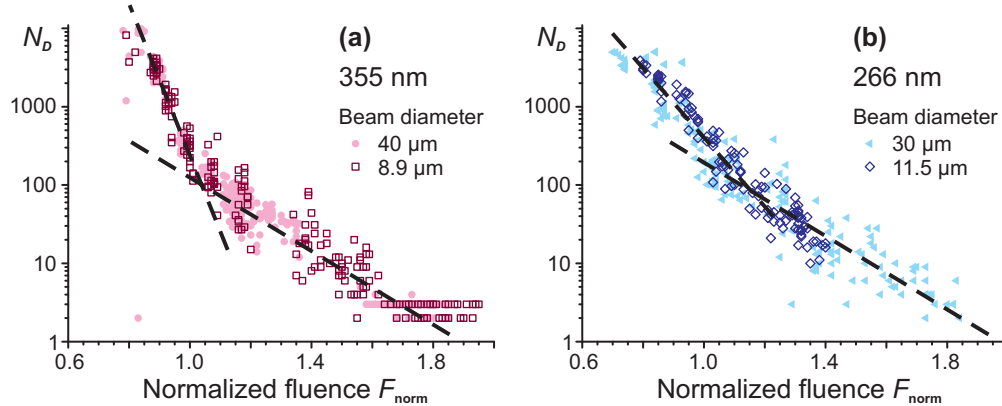


Fig. 4. Representation of the fatigue dynamics: number of pulses required to damage, N_d , as function of normalized fluence, F_{norm} . The fluence was normalized to the 50% damage threshold for 500 pulses. (a) Both beam sizes for 355 nm irradiation. (b) Both beam sizes for 266 nm irradiation. Dashed straight lines are guides to the eye.

5. Absolute threshold fluences for different beam sizes

In nanosecond laser-damage experiments, the absolute (not normalized) laser damage thresholds measured with smaller beams are typically higher than the ones obtained with larger beams [23, 24]. This observation made it difficult to compare measurements from different labs and was more or less solved for single pulse tests by understanding the laser damage probability as the probability that the high-fluence part of the laser beam encounters a damage precursor [25, 26].

Our data also show this effect of higher threshold fluences for smaller beams which is shown for 355 nm in Fig. 5. For 266 nm the difference is even higher reaching a factor of 3 when going from 30 μm to 11.5 μm .

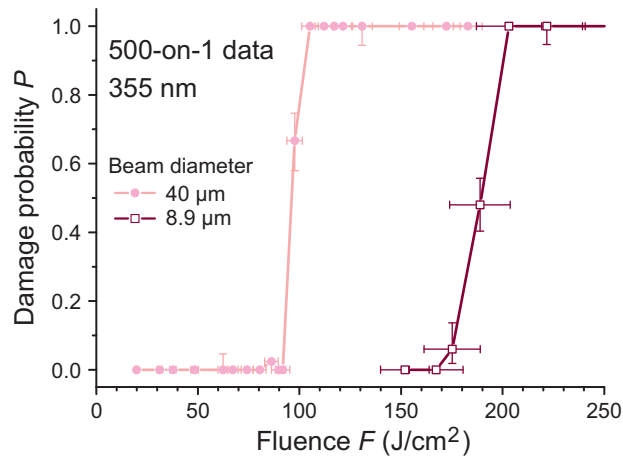


Fig. 5. S-on-1 damage probability data at 355 nm for both beam sizes and with a maximum of 500 pulses per site. The error bars in both directions are one-sigma error bars (68% confidence interval). The relative fluence uncertainty is obtained from fluctuations of the brightest pixel in the beam profile images (Fig. 2) and the probability error bars are calculated according to [27].

However, as we know that the measured laser-induced damage is dominated by light-induced cumulative material modifications, we cannot understand this effect as the probability

of encounter between the beam and homogeneously distributed damage precursors. As the beam itself generates the precursor (modifies the material) it will always find the precursor (hit modified material), and the probability of encounter is thus 100%.

The fact that the damage threshold is nevertheless higher for the smaller beams has thus to be understood by another model. Figures 5 and 3 (both close to step functions) indicate a deterministic nature of the damage initiation mechanism.

6. Lifetime of the material modifications

As our experiments were carried out at 50 Hz pulse repetition rate, defects of relatively short lifetime may contribute to the accumulating material modification. In order to get a first idea of the life-time of the defects that are relevant to laser damage initiation at 266 nm we mimicked the methodology applied non-destructively by Eva *et al.* to check the life-time of laser-induced absorption [28].

Two S-on-1 measurements were carried out, each of them including a break in the irradiation [Fig. 6(a)]. In each experiment, a fixed number of pulses, N_1 , was first sent on 10 different sites of the sample. Then, a break was made in the irradiation (7 minutes for the first series and 45 minutes for the second). After the break, the sites that were not damaged during the first part of the irradiation were irradiated again up to damage and the number of shots before damage, N_2 , was recorded.

Figure 6(b) compares both measurements with a break to a measurement without break (the latter represented as small yellow dots). Moreover, during the first experiment with a break of 7 minutes in the irradiation, four sites damaged before the end of the first series of 1000 shots, and are represented by green triangles in Fig. 6(b).

Supposing that the laser-created defects have a lifetime that is shorter than the break, one has only to take into account the number of shots received after the break, meaning that $N_D = N_2$. In this case, the first series of shots received by the sample before the break was totally “forgotten” by the material. Under this hypothesis, the data recorded in both break-experiments were depicted in Fig. 6(b), by means of dark blue crosses for the 7-minute-break experiment, and with purple daggers for the 45-minute-break experiment. These points appear clearly to be –in almost all cases– under the global trend followed by the yellow dots of the reference data.

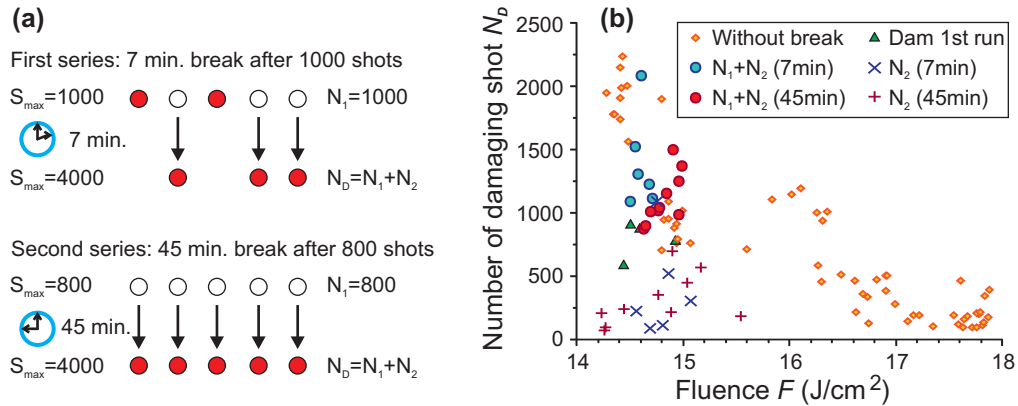


Fig. 6. **(a)** Schematic representation of both experiments carried out in the bulk of fused silica at 266 nm with a laser beam diameter of 30 μm with two different break durations in the irradiation: 7 minutes (first series) and 45 minutes (second series). For each site, the precise numbers of shots used during the first and the second part of the irradiation were recorded and are named N_1 and N_2 respectively. Red disks represent damaged sites and white disks undamaged ones (after the first part of the irradiation). **(b)** Number of shots needed to damage (N_D) as a function of the fluence. For more details, please refer to the text.

On the contrary, if one supposes that the laser-created defects are long-living enough to survive the breaks, N_D should be calculated taking into account the number of shots seen

before and after the break, and would thus be given by: $N_D = N_1 + N_2$. The results of this hypothesis are depicted in Fig. 6(b) by big blue and red disks for the 7-minute-break experiment and the 45-minute-break experiment respectively.

To conclude, we have highlighted by means of laser-induced damage tests that the lifetime of the damage-relevant defects generated at 266 nm in the bulk of fused silica were at least of 45 minutes, which is considerably longer than the time between two consecutive laser pulses (20 ms). Hence, defect accumulation is easily possible.

7. Discussion

The aim of multi-pulse laser damage studies in the material modification regime is to identify which is the light-induced material modification and by which physical process this modification lowers the laser damage threshold. The modification may possibly influence the propagation of the laser beam, so that the peak fluence inside the sample becomes higher than the peak fluence of the first pulse. Bosyi and Efimov showed that thermal self-focusing or formation of an index gradient 'lens' by material compaction may explain their experimental data in different irradiation conditions [8, 9]. The modification might also influence directly the absorption coefficient of the sample, for example by light-induced color center generation [9, 13]. Finally, it may also act on the mechanical yield strength of the material by introducing strain in the vicinity of the material modifications (color centers, compaction zone) [13]. Naturally all these effects may appear simultaneously with different relative importance, which leads to a large number of possible fatigue mechanisms.

The presented data shows that multiple-pulse laser-damage in the bulk of Suprasil 1 at 355 nm and at 266 nm is governed by cumulative material modifications that are induced by the irradiation (Fig. 3 and Fig. 3 in [15]). This is in fact expected at wavelengths of 248 nm (5.00 eV) and below, where synthetic fused silica is known for UV-induced absorption even at small fluences (per pulse) [2, 28, 29]. At longer wavelengths (266 nm [16], 308 nm [29] and 353 nm [17]) no build-up of laser-induced linear absorption was revealed for small fluences in synthetic fused silica. However, the fluences used in our study are much higher and electronic excitation by three-photon absorption (for 355 nm, 3.49 eV) or two-photon absorption (for 266 nm, 4.66 eV) is possible considering a band gap of 8.52 eV for synthetic fused silica [30].

The life-time of damage-relevant defects at 266 nm was found to be longer than 45 minutes. A value that recalls the result of Eva *et al.* at 248 nm where the lifetime of the light-induced absorption was found to be more than 12 hours [28]. It is thus possible that the defects involved in damage initiation at 266 nm are identical to those observed non-destructively through laser-induced absorption at 248 nm [2, 28, 29] and 193 nm [28, 29]. They are however different from accumulating defects in lead silicate glass that revealed a lifetime of less than 7 minutes in the same type of test [9].

In our study we used two different beam sizes at both wavelengths and all beam shapes were rather far from the ideal TEM₀₀ Gaussian shape (Fig. 2). As the defects that lead to laser damage (laser damage precursors) are generated by the beam itself, the 1-on-1 models based on a distribution of preexisting damage precursors and the probability of encounter between the spatially homogeneously distributed damage precursors and the high-fluence region of the beam [26] cannot be applied. An analytical description of the beam shape is thus not of prime importance for the analysis of our data. However, our data also show that the beam size, and possibly the beam shape are nevertheless important to the damage mechanism.

At a given wavelength the $N_D(F)$ -data for the two different beam sizes only differs by a scaling factor for the fluences (Fig. 4). In other words, at a given normalized fluence the lifetime in terms of number of pulses before damage is the same for both beam sizes. This is an important difference to similar experiments in lead silicate glass [8, 9], where the material modifications occurring during S-on-1 damage tests were found to induce beam propagation effects in the following pulses. Depending on the wavelength, the authors proposed thermal self-focusing and densification-induced self-focusing. In consequence, we can say that the

material modifications in our experiments do not generate important beam propagation effects for the following pulses.

For each tested wavelength (266 nm and 355 nm), the $\log(N_D)$ representation as a function of normalized fluence F_{norm} (Fig. 4) can be approximated by two straight lines with different slopes. Moreover, the slope of the line at high fluence and small pulse number is the same for 355 nm and 266 nm. The slope of the straight line for low fluences and high pulse number is steeper especially at 355 nm. These two slopes may correspond to two different defects generated by the irradiation, as suggested in articles dealing with the dynamics of laser-induced absorption at shorter wavelengths [2, 28]. As outlined in the laser-induced absorption studies, the different defects are not independent from each other but the defects responsible for laser damage at low fluence (type 1) are converted to the second type of defects at higher fluence which in fact makes the material more resistant compared to the existence of defect type 1 only. As we do not yet have non-destructive measurements of the generated defects and their densities, it is difficult to give a more detailed interpretation, even if the two most probable defect types regarding the literature are E' centers and NBOHC [2]. Nevertheless, as mentioned before, these defects are reported in literature only for shorter wavelengths, than those we use, but in our irradiation conditions they could be created by multi-photon absorption (see next paragraph). Once generated, the defects may absorb single laser photons and, by passing through an electronically excited state, they may convert to other defects like oxygen deficiency centers (ODC(II)) [3, 4, 31]. Nevertheless this hypothetical mechanism needs confirmation through spectroscopic measurements of the modified but not yet damaged material in the low and high fluence regimes.

The absolute 500-on-1 thresholds for similar beam size at 355 nm (diameter 40 μm) and 266 nm (diameter 30 μm) differ approximately by a factor of 9. 1-on-1 measurements by Kuzuu et al revealed also a strong difference between these two wavelengths [32]. This strong difference is probably a consequence of the different order of multi-photon absorption necessary to cross the band gap of fused silica at the two wavelengths.

Finally, despite the fact that the beam itself produces the defects, the threshold fluence for smaller beams is higher than for larger beams (Fig. 5). Bosyi and Efimov reported the same observation [9] but did not comment on it. In order to discuss this observation we might exclude some simple theories. First, heat conduction away from the heated focal region during the pulse duration is more significant if the heated region is smaller. However the typical heat conduction length $l_T = 2\sqrt{D\tau}$, with D the heat diffusivity and τ the pulse duration [33], is only 0.16 μm for fused silica ($D = 8.1 \cdot 10^{-7} \text{ m}^2/\text{s}$ below 100°C [34]) and for a pulse duration of 8 ns. Thus lateral heat conduction out of the focal volume is negligible during the pulse duration considering the used beam sizes. The peak temperature reached by an absorber in the focal region, irradiated at a given fluence, is thus nearly independent of the used beam. Secondly, one might think that we deal in fact with many small absorbers that might form clusters and thus the cluster formation should be different for small beams compared to large beams. However, the possible sites where the defects can be created in the material are so close (some atom distances) that, again, the used laser beam sizes appear huge. Additionally to this qualitative consideration, we may compare the situation to Monte-Carlo type simulations on laser damage in KDP that used a cell size of one by one micron square and that was able to perfectly explain laser damage results obtained with rather large laser beams [35]. Hence, clustering of the defects cannot explain the observed differences between the used beam sizes either.

Thus, we think that the fact that higher damage thresholds are measured with smaller beams is rather linked to electronic or electrostrictive self-focusing mechanisms during the pulse initiating laser-damage. Describing nonlinear self-focusing in an analytical way always involves a critical laser beam power [36]. This critical power for strong nonlinear self-focusing is a material constant and is reached at lower intensity for larger beams compared to smaller beams. This means in agreement with our observations that strong self-focusing, leading to damage, will be reached at lower fluences for larger beams. Thus, the critical

modification that the irradiation causes in the material, is an increase in the nonlinear refractive index, as it has been reported before in nonlinear optical crystals [37]. The fact that we do not observe an influence of the modifications on the propagation of the beam is probably due to the bad pointing stability of the laser. The laser-induced modifications will be rather homogeneous in a region larger than the beam size because each pulse irradiates a slightly different volume. As a consequence, the beam propagates through an approximately homogeneous material that however increases its nonlinear refractive index until catastrophic self-focusing occurs.

To conclude, the preliminary scenario we propose for UV multiple-pulse damage initiation in the bulk of Suprasil 1 is thus the following one: 2- or 3-photon absorption (depending on the wavelength) generates electron-hole pairs, the relaxation of which may create two types of defects, depending on the fluence range. The existence of these defects during irradiation with the subsequent laser pulses will have at least two effects: (i) absorption is increased leading to a temperature rise that enables annealing of the defects at a small rate, (ii) the conditions for electronic or electrostrictive self-focusing are improved which finally leads to laser damage. The safe fluence is thus the fluence at which annealing of the defects is able to compensate for the newly generated defects, ensuring low enough defect concentration to avoid catastrophic self-focusing. Further modeling work and spectroscopic measurements are however required to confirm the proposed scenario.